Propagation properties of density pulses and ion acoustic waves in collisionless plasmas calculated from the linearized Vlasov equation

Jensen, V.O.

Publication date:
1972

Document Version
Publisher's PDF, also known as Version of record

Risø Report No. 257

Risø Report No. 257

Danish Atomic Energy Commission

Research Establishment Risø

Propagation Properties of Density Pulses and Ion Acoustic Waves in Collisionless Plasmas Calculated from the Linearized Vlasov Equation

by V. O. Jensen and P. Michelsen

February 1972

Sales distributors: Jul. Gjellerup, 87, Sølvgade, DK-1307 Copenhagen K, Denmark

Available on exchange from: Library, Danish Atomic Energy Commission, Risø, DK-4000 Roskilde, Denmark

U. D. C.
533.9

February 1972 Risø Report No. 257

Propagation Properties of Density Pulses and Ion Acoustic Waves in Collisionless Plasmas Calculated from the Linearized Vlasov Equation

by

V. O. Jensen and P. Michelsen

Danish Atomic Energy Commission
Research Establishment Risø, Roskilde, Denmark

Abstract

Calculations of the propagation properties of ion density perturbations and waves through collisionless plasmas with Maxwellian velocity distribution functions are presented. The calculations are based on the linearized Vlasov equation, which is solved with the perturbation as a boundary value. Solutions are presented for various values of the ratio between electron and ion temperature and for various drift velocities of the background plasma and of the perturbations at the boundary. Some of the results are compared with those obtained in a simple Landau treatment of the problem.

ISBN 87 550 0132 7

CONTENTS

I. INTRODUCTION

Propagation of ion density perturbations through collisionless plasmas has been studied intensively in recent years. The main purpose has been to verify experimentally theoretical results obtained from calculations based on the linearized Vlasov equation. In most cases the theoretical calculations have been performed under various simplifying assumptions and approximations. Arguments against the validity of the obtained results and the conclusions drawn after comparing them with experiments have been raised by several authors [1-5] in recent years.

In this paper we consider an infinite homogeneous plasma with density n_o and calculate propagation properties of longitudinal density perturbations along a constant magnetic field (B = 0 also included). We describe the electrons by their fluid equation

$$E = - \frac{\varkappa T_e}{q} \frac{1}{n_o} \frac{\partial n(x,t)}{\partial x} \tag{1}$$

and assume quasi-neutrality, $n_i = n_e$. The linearized Vlasov equation for the ions can thus be written

$$\frac{\partial f(x,v,t)}{\partial t} + v \frac{\partial f(x,v,t)}{\partial x} = c_e^2 \frac{1}{n_o} \frac{df_o(v)}{dv} \frac{\partial n(x,t)}{\partial x} \tag{2}$$

where

$$c_e^2 = \varkappa T_e/m_i, \quad n(x,t) = \int_{-\infty}^{\infty} f(x,v,t)\, dv$$

and where the ion velocity distribution function, $f_o(v)$, of the background plasma is related to n_o through

$$n_o = \int_{-\infty}^{\infty} f_o(v)\, dv \ .$$

The equations (1) and (2) are valid for slow ($t \gg \omega_{pi}^{-1}$) and long wavelength ($\lambda \gg \lambda_{Debye}$) phenomena, such as propagation of ion acoustic waves and density perturbations in Q-machines and many other steady-state plasmas.

We consider density perturbations excited at x = 0 by some source (grid, photo ionization, electron beam ionization, etc.), and propagating

through the background plasma along the x-axis. The ion velocity distribution function in the source-generated perturbation at $x = 0$ is called $g(v)$. Thus $|v|g(v)$ is proportional to the number of ions with velocity v created or absorbed per time unit by the source. In this paper we consider two kinds of perturbations: a) short pulses generated by activating the source during a short time ($\delta(t)$), and b) sine waves generated by activating the source by an oscillating signal.

The mathematical procedure used in calculating the propagation properties for the short pulses has been described elsewhere [4]. It was found that pulses propagate in a self-similar manner, i.e. that the perturbed density n and the perturbed ion velocity distribution function f can be written as

$$n(x,t) = \frac{1}{t}\, h\left(\frac{x}{t}\right) \tag{3}$$

and

$$f(x,v,t) = \frac{1}{t}\, k\left(\frac{x}{t},\ v\right) , \tag{4}$$

where t is the time after the pulse was released at $x = 0$.

The functions h and k are calculated from (2), and are found to depend on $f_o(v)$, on $g(v)$ and on the electron temperature.

Although most interest, experimentally and theoretically, has been devoted to waves, propagation properties of a pulse much more clearly reveal the physical phenomena, such as wave-particle interaction described by (2) [4, 7]. Furthermore propagation of short pulses is interesting because the functions (3) and (4) are nothing but the Green's functions of equation (2) and they can therefore be used to calculate propagation properties of waves [6] and all other kinds of perturbations. From the Green's functions considerable physical insight into wave phenomena can be gained.

In calculating the propagation properties of waves we have used the technique described in ref. 5. This technique is mathematically the same as to perform convolution integrals of the Green's functions. We have calculated the amplitude, amp_n, and the phase, φ_n, of the wave density as functions of the dimensionless distance, $x\omega/c_i$, from the source. In some cases we have also calculated the amplitude, amp_f, and the phase, φ_f, of the perturbed ion velocity distribution function for various values of the velocity v.

In this report we give results obtained for cases where $f_o(v)$ and $g(v)$ are drifting Maxwellians of the form,

$$f_o(v) \propto \exp(-(v-v_d)^2/c_i^2) \qquad (5)$$

and

$$g(v) \propto \exp(-(v-v_{dg})^2/c_{ig}^2) \ . \qquad (6)$$

v_d and v_{dg} are the drift velocities of the background plasma and of the perturbation, respectively. c_i is related to the ion temperatures through $c_i^2 = 2\varkappa T_i/m_i$, and similarly $c_{ig}^2 = 2\varkappa T_{ig}/m_i$. The propagation properties are calculated for various values of the parameters $\vartheta = T_e/T_i$, v_d/c_i, v_{dg}/c_i and T_i/T_{ig}. We also present a few results obtained for cases where $f_o(v)$ and $g(v)$ consist of two drifting Maxwellians (double-humped function).

As a starting point we take the case $v_d = v_{dg} = 3c_i = 3c_{ig}$ and present detailed calculations for various ϑ-values. We then change the parameters around this standard case and discuss a comparison between the obtained results. Throughout the report we try to give a physical explanation of the shapes of the calculated curves. A survey of the cases treated is seen in table I.

II. RESULTS

Figs. 1 to 5 show propagation properties of pulses and waves through our standard plasma with parameters: $v_d = v_{dg} = 3c_i = 3c_{ig}$. The temperature ratio, T_e/T_i, is varied from one figure to another. The density in a pulse propagating into a plasma with $T_e = 0$ is shown in fig. 1a). This is the case of freely streaming ions (rhs-side in equation (2) = 0) where the propagation is determined only by the distribution, g(v), in the density pulse generated at the source. Fig. 1b) shows calculated values of the perturbed ion velocity distribution function for three v-values. In calculating the f-function, we have assumed that these functions are measured experimentally with an electrostatic ion energy analyser, which has a resolution in velocity equal to $c_i/4$ [4].

As the temperature ratio T_e/T_i is increased (figs. 2 to 5) the collective interaction term (rhs-side term in equation (2)) starts to be of importance. We note an increase in pulse velocity in the figures marked a) and an undershoot on the f-curves in the figures marked b). This latter feature is easy to demonstrate experimentally [4, 7]. At high temperature ratios, we notice furthermore a tendency for the pulses to split up into two (see also the insert in fig. 5a)); this phenomenon has been explained elsewhere [6].

The rather complicated shape of the f-curves in fig. 5b) can be understood physically by arguments as those used to explain the undershoot in ref. 7.

Figs. 1c) to 5c) show as functions of $x\omega/c_i$ the amplitude, amp_n, and the phase, φ_n, of the density in waves generated by activating the source with a frequency ω. For the case of freely streaming ions shown in fig. 1, the damping of the wave is caused by phase mixing; in this case it does not approach an exponential curve for large $x\omega/c_i$. With increasing temperature ratios the damping rate increases close to the grid, but for large $x\omega/c_i$ - values we find a continuously weaker damping and that the amplitude approaches an exponentially damped curve. In table I a comparison is given between our results and those obtained by solving the problem by considering only the first pole in a simple Landau treatment. The oscillating nature of the amplitude seen for $x\omega/c_i$ up to about 20 in figs. 3c) and 4c) is caused physically by a beating between a slow wave and a fast one associated with the slow and the fast pulses just discussed.

Finally figs. 1d) to 5d) show the amplitude, amp_f, and the phase, φ_f, of the perturbed ion velocity distribution function in a wave. amp_f and φ_f are also calculated as functions of $x\omega/c_i$ and they are shown for three v-values. In the case of freely streaming ions in fig. 1d) the amplitude is of course constant and the phase increases proportionally to the distance from the source ($f(x,v) = g(v)\exp(i\omega x/v)$). As the temperature ratio is increased we note oscillations in the amplitude and the phase curves. These oscillations are caused by collective effects and can be understood by simple physical arguments as those used in ref. 7.

At high T_e/T_i-values (order 5 to 10) our code used in computing propagation properties of waves is not very accurate for small $x\omega/c_i$-values; we have indicated this lack of accuracy by dotting the curves in figs. 5c) and 5d).

It is also of interest to know the amplitude and the phase of the perturbed ion velocity distribution function f(v) in a wave at various distances from the source. Figs. 6 to 8 show these quantities calculated for our standard plasma for three T_e/T_i-values. In the case $T_e/T_i = 0$ as in fig. 6 the amplitude of f(v) is given by the distribution, g(v), in the perturbation excited at the source and it is independent of distance from source. The phase is also simple as it is proportional to $x\omega/v$. The phase is shown in fig. 6 as a function of v/c_i calculated at three distances from the source.

Fig. 7 shows the amplitude of f(v) calculated at three distances from the source for $T_e = T_i$. Only a very small difference between the amplitude

curves in fig. 7 and those in fig. 6 is noticed. The phase curves for $T_e = T_i$ (not shown in fig. 7) coincide nearly completely with those in fig. 6 obtained for $T_e = 0$.

In fig. 8 we treat the case $T_e = 5\ T_i$. Here we note a clear difference from the case of freely streaming particles in fig. 6 as a pronounced oscillation in the $amp_{f(v)}$-curves. The curves in fig. 8a) to 8d) are calculated for four values of $x\omega/v$. Again in this case the φ_n-curves are very similar to those shown in fig. 6 and therefore not shown.

The oscillations in the $amp_{f(v)}$-curves in fig. 8 are clearly caused by collective interactions. The following arguments explain the oscillations physically. When f(v) is measured at a fixed position, we expect that collective interaction between source and point of measurement will cause a periodicity in f(v) with a period in v-space which is determined by the velocity of those particles that have crossed an entire number, N, of wavelengths between source and point of measurement. An ion with the velocity, v_N, has crossed N wavelengths if

$$v_N = \frac{v_{phase}}{1 + N \frac{2\pi v_{phase}}{\omega x}} \qquad (7)$$

where v_{phase} is the phase velocity of the wave and N is an integer

$$\left(- \frac{x\omega}{2\pi v_{phase}} \leq N < + \infty \right).$$

Furthermore, because the collective term is proportional to $df_0(v)/dv$ we expect a phase shift of 180° around that v-value for which $df_0(v)/dv = 0$. From equation (7) we note:

a) the period in the oscillation in f(v) decreases with increasing N, i.e. with decreasing velocity,

b) the period decreases with distance from the source.

For the case treated in fig. 8 $v_{phase} = 5.1\ c_i$. A comparison between the calculated curves in fig. 8 and equation (7) shows complete agreement.

Similar oscillations in f(v) have been found in calculations by Buzzi [8]. As the oscillations are direct signature of collective particle-wave interaction, it would be very interesting to demonstrate them experimentally. The very simple dependence of distance given by equation (7) would facilitate such an experiment.

The curves in figs. 1 to 8 are calculated for our standard case: $v_d = 3c_i$, $v_{dg} = 3c_i$ and $T_i = T_{ig}$. We now show some examples of what happens when these parameters are changed independently. In the following we only present curves showing the propagation of the density of short pulses (marked a) and curves showing the amplitude, amp_n, and the phase, φ_n, of waves (marked b). In the calculations shown in figs. 9 to 11 we have chosen the drift velocity of the undisturbed plasma $v_d = 2c_i$ and kept $v_{dg} = 3c$ and $T_i/T_{ig} = 1$ as in the standard case. In the case of $T_e = 0$ we of course obtain the same results as for the standard case. Hence we give results only for relatively high T_e/T_i-values. Fig. 9 treats the case $T_e/T_i = 2$. We notice that the pulse shown in fig. 9a) moves with a slower velocity than the one in the standard case calculated for the same temperature ratio and shown in fig. 4a). This is to be expected because the drift velocity of the background plasma is now decreased. For the same reason the phase velocity, as deduced from the φ_n-curves in fig. 9b), is lower than that deduced from fig. 4c. We also note that we do not see the tendency for the pulses to split up into two as in the standard case. This is because the slow pulse moves against the drift of the background plasma; only when the propagation velocity of this pulse is lower than the drift velocity of the background plasma as in the standard case we see the pulse for $x > 0$. For the same reason we have no slow wave propagating and therefore we do not have an oscillating nature in the amp_n-curve in fig. 9b as was the case in fig. 3c, Figs. 10 and 11 show the corresponding curves for $T_e/T_i = 5$ and 10, respectively. The discussion just given is also valid for the figures.

In figs. 9 to 11 we showed the effect of changing the drift velocity, v_d, of the background plasma. We now turn to the situation when the drift velocity, v_{dg}, of the source-induced perturbation is changed. Again we confine ourselves to relatively high T_e/T_i-values, where collective interaction is of importance. The results are shown in figs. 12 to 17.

For the cases treated in figs. 12 to 14 the drift velocity, v_{dg}, in the source-induced perturbation is below that of the background plasma. We notice on all three figures that the pulses again split up into two: one with a velocity essentially equal to v_{dg} and a fast one with a velocity that increases with T_e/T_i. It is an interesting feature to note that the perturbed density goes negative between the two pulses. Having realized that the pulse splits up into two in this case it is possible to understand physically that the perturbed density can go negative between the pulses. The majority of the ions in the background plasma have velocities around v_d, i. e. velocities

between those of the two pulses. Therefore the ions in the background plasma running between the two pulses have been overtaken by the fast pulse and thus received a net acceleration; furthermore, when close to the slow pulse, these ions are acted upon and accelerated by the field associated with this pulse [7]. Therefore the velocity of these ions is increased and, because of the equation of continuity $n \langle v \rangle = \text{const}$, n has to decrease.

In the case of waves we expect a pronounced effect of beating between the waves associated with the slow and the fast pulse. In figs. 12b to 14b we see that this beating causes a strong oscillation in the wave amplitude and also in the phase.

The curves shown in figs. 15 to 17 are calculated for cases where v_{dg} is above the drift velocity of the background plasma. In this case we preferentially excite the fast ion acoustic pulse and not the slow one. The density pulse is therefore very narrow and it goes negative after the main pulse for the same reason as discussed above. In the case of waves the oscillating nature of the amplitude (see figs. 15b to 17b) is much less than in figs. 12b to 14b. (Note the change in the abscissa scale).

Finally, in figs. 18 to 23 we show the effect of changing the width of the distribution function g(v). We keep $v_d = v_{dg} = 3c_i$ as for the standard case and look first at the case $T_i/T_{ig} = 5$, i. e. at the case where g(v) is a very narrow distribution function. The shape of the density pulse for the case of freely streaming ions as shown in fig. 18a is of course much narrower than in the corresponding standard case as shown in fig. 1a. As the temperature ratio T_e/T_i is increased as in figs. 19a and 20a, the shape of the density curve for pulses changes. We first notice a weak knee on the curve for $T_e/T_i = 1$, and for $T_e/T_i = 5$ (fig. 20a) we have three maxima on the curve or three separate pulses propagating. The slow and fast pulses can be interpreted as ion acoustic pulses as already discussed. The pulse between them is made up of the ions in the source-induced perturbation; the contribution from these ions now appears as a separate pulse because the spread in g(v) is very small. When we look at the amp_n-curves in figs. 21b we again notice the tendency for a strong oscillation in amp_n to occur when the density in the short pulses has two or more maxima.

When we turn to the case where g(v) is a very wide function as in figs. 21 to 23, which are calculated for $T_i/T_{ig} = 0.2$, we do not see the contribution from the ions in g(v) as a single pulse any more. By comparing the amp_n-curves in fig. 20b) and fig. 23b) we see that the oscillating nature does not depend very much on whether the density curve for the pulse has two or three maxima.

In experiments in single-ended Q-machines one often has an ion velocity distribution function in the background plasma with two maxima [3]. We therefore also treat such plasma; in the calculation we have chosen $f_o(v)$ to have the form

$$f_o(v) = \text{const} \left[\exp(-(v-v_{d1})^2/c_i^2) + \exp(-(v-v_{d2})^2/c_i^2) \right] . \qquad (8)$$

We present calculations of the density in short pulses and of amp_n and φ_n for waves for two cases. In fig. 24 the parameter values are $v_{d1} = c_i$, $v_{d2} = 3c_i$, $v_{dg} = 3c_i$, $T_i = T_{ig}$ and $T_e/T_i = 1$. In fig. 25 we have used the same parameters except that $T_e/T_i = 5$. A comparison between the curves in fig. 24 and the corresponding ones in fig. 3 shows that the propagation properties for pulses and waves in a plasma with $T_e = T_i$ are rather unaffected by the shape of $f_o(v)$. This is because the collective interaction is weak at these relatively low T_e/T_i-values. When T_e/T_i is increased to 5 as in fig. 25 we note a considerable change: the pulse splits up into two, a fact which for the case of waves causes a very strong oscillation in the amp_n-curve.

In many experimental situations as for instance in grid excitation of waves and pulses in single-ended Q-machines [9] the distribution function in the source-induced perturbation differs from a Maxwellian. We now show the effect of changing g(v) from a simple Maxwellian to a distrbution function with two maxima of the form

$$g(v) = \text{const} \left[\exp(-(v-v_{dg1})^2/c^2) + \exp(-(v-v_{dg2})^2/c_i^2) \right] . \qquad (9)$$

We have performed the calculations for $v_d = 3c_i$ as in the standard case. For the drift velocities of the two humps in g(v) we have chosen $v_{dg1} = c_i$ and $v_{dg2} = 3c_i$, respectively. Fig. 26a shows the propagation of a pulse for the case $T_e/T_i = 0$. We note that the result is very similar to that obtained for the standard case and shown in fig. 1a except for a relatively higher density at large tc_i/x-values. This is caused by the slow ions in g(v) which appear after the main pulse. As the temperature ratio is increased as in figs. 27a and 28a we notice a much stronger tendency for the pulse to split up into two than for the standard case. This is because the ions in the slow hump in g(v) preferentially excite the slow pulse. As discussed before, when a pulse has a strong tendency to split up into two, the amplitude of a wave will have a strong oscillating nature; this effect is seen very pronounced in fig. 28b.

III. DISCUSSION AND CONCLUSIONS

In this work we have presented exact numerical calculations of the propagation properties of pulses and waves through collisionless plasmas. We have shown that the propagation depends very strongly on the velocity distribution function in the background plasma, on the velocity distribution in the source-induced perturbation and on the temperature ratio T_e/T_i. It is probably most interesting to note that the wave amplitude oscillates in many cases. As our calculations are based on the linearized Vlasov equation (2), such oscillations, when seen experimentally, should not mistakenly be interpreted as being caused by nonlinear effects. The calculations also show that the difference in propagation properties between the case of freely streaming ions ($T_e/T_i = 0$) and the case with collective interaction ($T_e \neq 0$) is not always very pronounced. Therefore it is offhand difficult to think out experiments that clearly demonstrate the effect of the collective interaction term in equation (2). The undershoot seen on the curves in figs. 2b to 5b is caused by collective interaction [7] and has been seen experimentally [4]. For the wave case the oscillations in the $amp_{f(v)}$-curves shown in figs. 7 and 8 are also clear effects of collective interaction. With known technique [4] it should be possible to see such oscillations experimentally. Because they have a very characteristic dependence on distance from source as given by equation (7), an experimental observation of this dependence would provide a clear-cut signature of collective interaction.

We have confined ourselves to present calculation of amp_n and φ_n for $x\omega/c_i$-values up to 50 (except in figs. 15 to 17). In most cases, as is evident from the curves, $x\omega/c_i = 50$ corresponds to 2 to 3 wavelengths so we consider only the "near field".

Traditionally (see ref. (10)) calculations of wave propagation have been simplified by considering only the dielectric function

$$\varepsilon(k,\omega) = 1 - d_e^2 \omega_{pi}^2 k \int \frac{f_o'(v)}{kv-\omega}\, dv = 1 - \frac{T_e}{T_i}\ \frac{1}{2} Z'\left(\frac{\omega/k \pm v_d}{c_i}\right), \tag{10}$$

where d_e is the electron Debye length and Z is the plasma dispersion function [11].

By solving the equation $\varepsilon(k,\omega) = 0$, one gets a number of (k,ω)-values, each of which corresponds to a Landau mode of the form $\exp(-i(\omega t - kx))$.

discussion of the validity of this approximation was given by Gould [12]. We have solved the equation $\varepsilon(k, \omega) = 0$ for the cases presented in the figures in this report. From the "first pole" [10] we have calculated the phase velocity, v_{ph}, and the damping rate δ/λ. In table I we compare the results of the first pole approximation with exact calculations of the same quantities performed for $x\,\omega/c_i \approx 50$.

The signature ~ in front of the calculated δ/λ-values indicates that we see a strong change in this quantity with $x\,\omega/c_i$ around $x\,\omega/c_i = 50$. It is evident from table I that the "first Landau pole" approximation generally does not lead to a solution with satisfactory accuracy. On the whole the agreement between our results and those obtained with the "first pole" approximation gets worse at lower $x\,\omega/c_i$-values. We may therefore conclude that the "first Landau pole" approximation is dissatisfactory for calculations of propagation properties of waves in the near field [12], (< 2-$3\,\lambda$), where experiments are normally done [10]. Details in the exciting mechanism is as important for the wave as the dielectric properties of the plasma.

REFERENCES

1) R. W. Gould, Phys. Rev. 136, A991 (1964).

2) J. L. Hirshfield and J. H. Jacob, Phys. Fluids 11, 411 (1968).

3) S. A. Andersen, V. O. Jensen, P. Michelsen, and P. Nielsen, Phys. Fluids 14, 728 (1971).

4) S. A. Andersen, G. B. Christoffersen, V. O. Jensen, P. Michelsen, and P. Nielsen, Phys. Fluids 14, 990 (1971).

5) G. B. Christoffersen, V. O. Jensen, and P. Michelsen, Proceedings of the 3rd Int. Conf. on Quiescent Plasmas, Elsinore, Sept. 20-24, 1971, Risö Report No. 250, p. 63 (1971).

6) V. O. Jensen, Proceedings of the 3rd Int. Conf. on Quiescent Plasmas, Elsinore, Sept. 20-24, 1971, Risö Report No. 250 (1971), p. 87.

7) S. A. Andersen, V. O. Jensen, P. Michelsen, and P. Nielsen, Phys. Letters 32A, 413 (1970).

8) J. M. Buzzi, Proceedings of the 3rd Int. Conf. on Quiescent Plasmas, Elsinore, Sept. 20-24, 1971, Risö Report No. 250, p. 40 (1971).

9) G. B. Christoffersen, Proceedings of the 3rd Int. Conf. on Quiescent Plasmas, Elsinore, Sept. 20-24, 1971, Risö Report No. 250, p. 55 (1971).

10) A. Y. Wong, R. W. Motley, and N. D'Angelo, Phys. Rev. 133, A436 (1964).

11) B. D. Fried and S. D. Conte, The Plasma Dispersion Function (Academic Press Inc., New York, 1961).

12) R. W. Gould, Phys. Rev. 136, A991 (1964).

					Our results for $\alpha = \omega/c_1 = 50$		Results from "first pole" approximation	
Fig.	T_2/T_1	v_d/c_1	v_{dg}/c_1	T_1/T_{1g}	v_{ph}/c_1	b/λ	v_{ph}/c_1	b/λ
1	0.0	3	3	1	4.25	0.49	undefined	
2	0.5	3	3	1	4.36	0.82	4.41	0.84
3	1.0	3	3	1	4.47	1.25	4.53	1.18
4	2.0	3	3	1	4.68	1.85	4.72	1.85
5	10.0	3	3	1	5.88	~10	5.86	31.7
6	0.0	3	3	1	4.25	0.49	undefined	
7	1.0	3	3	1	4.47	1.25	4.53	1.18
8	5.0	3	3	1	5.12	~5	5.13	4.97
9	2.0	2	2	1	3.71	1.5	3.73	1.46
10	5.0	2	2	1	4.13	~4	4.14	4.00
11	10.0	2	2	1	4.86	~15	4.86	17.0
12	1.0	3	1	1	4.66	1.5	4.53	1.18
13	2.0	3	1	1	4.86	~2.5	4.97	2.06
14	5.0	3	1	1	5.12	~4	5.13	4.97
15	1.0	3	5	1	5.08	1.4	4.53	1.18
16	2.0	3	5	1	5.17	1.9	4.97	2.06
17	5.0	3	5	1	5.35	~20	5.13	4.97
18	0.0	3	3	5	8.20	1.0	undefined	
19	1.0	3	3	5	2.9	~1	4.53	1.18
20	5.0	3	3	5	4.8	~4.7	5.13	4.97
21	0.0	3	3	0.2	0.48	~0.4	undefined	
22	1.0	3	3	0.2	4.58	0.7	4.53	1.18
23	5.0	3	3	0.2	5.25	2.5	5.13	4.97
24	1.0	$\left\{\begin{matrix} v_{d1}/c_1 = 3 \\ v_{d2}/c_1 = 1 \end{matrix}\right\}$	3	$T_{11} = T_{12} = T_{1g}$	4.44	~0.9	2.15	0.80
25	5.0	$\left\{\begin{matrix} v_{d1}/c_1 = 3 \\ v_{d2}/c_1 = 1 \end{matrix}\right\}$	3	$T_{11} = T_{12} = T_{1g}$	3.9	~3.5	2.01	0.214
26	0.0	3	$\left\{\begin{matrix} v_{dg1}/c_1 = 1 \\ v_{dg2}/c_1 = 3 \end{matrix}\right\}$	$T_1 = T_{1g1} = T_{1g2}$	4.24	~0.5	undefined	
27	1.0	3	$\left\{\begin{matrix} v_{dg1}/c_1 = 1 \\ v_{dg2}/c_1 = 3 \end{matrix}\right\}$	$T_1 = T_{1g1} = T_{1g2}$	4.50	1.3	4.53	1.18
28	5.0	3	$\left\{\begin{matrix} v_{dg1}/c_1 = 1 \\ v_{dg2}/c_1 = 3 \end{matrix}\right\}$	$T_1 = T_{1g1} = T_{1g2}$	5.1	3.7	5.13	4.97

Table I

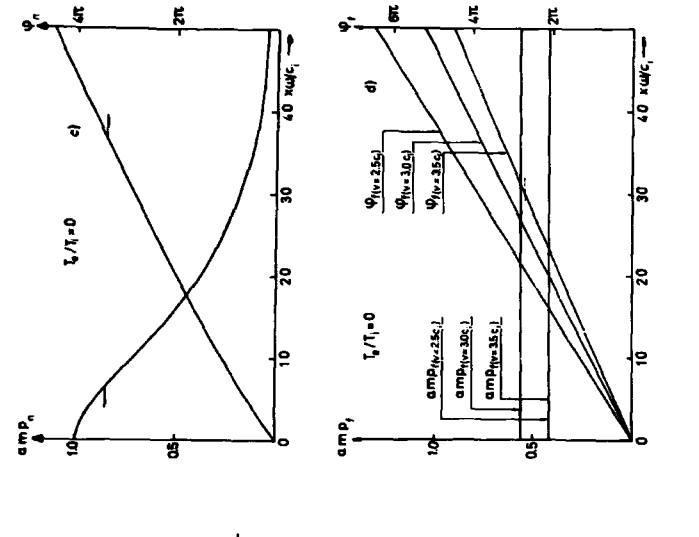

Fig. 1. a) and b) propagation of pulses, c) and d) propagation of waves.
$T_e/T_i = 0$, $v_{gr}/c_i = 3$, $v_{gr}/c_i = 3$, $T_i/T_{iE} = 1$.

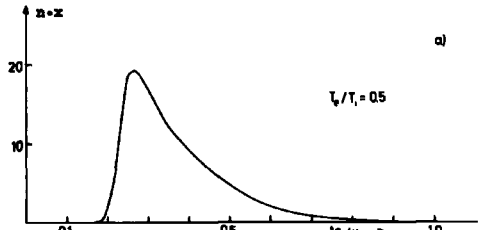

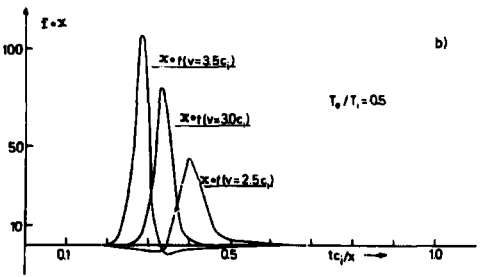

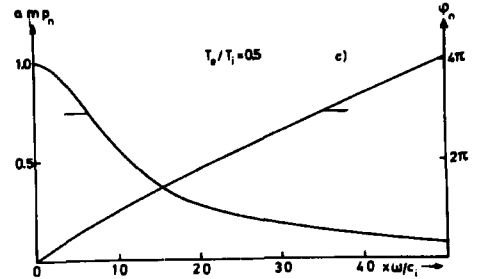

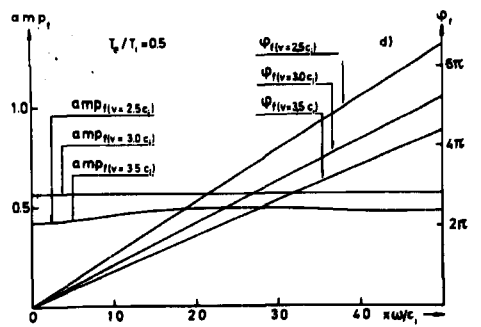

Fig. 3. a) and b) propagation of pulses, c) and d) propagation of waves.
$T_e/T_i = 0.5$, $v_d/c_i = 3$, $v_{dg}/c_i = 3$, $T_i/T_{ig} = 1$.

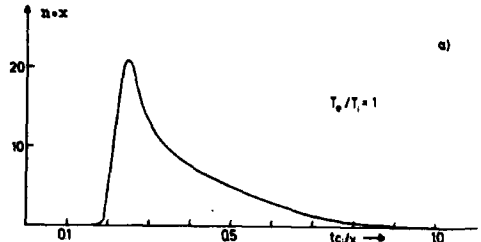

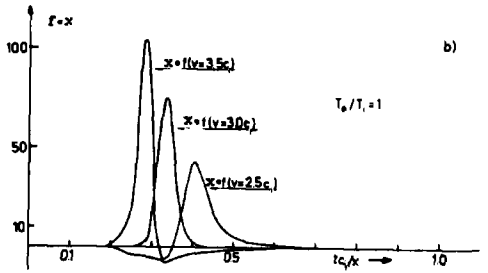

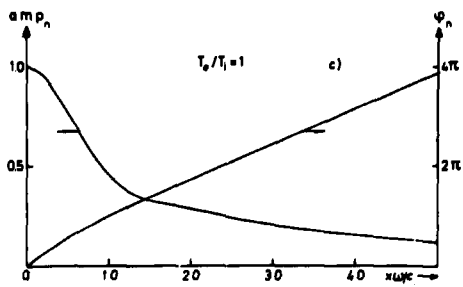

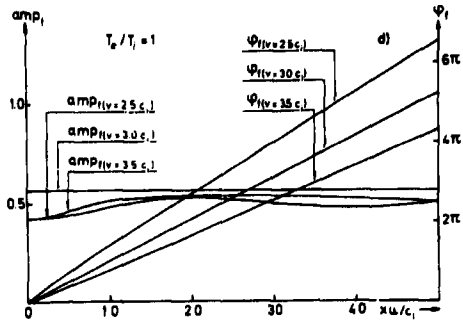

Fig. 3. a) and b) propagation of pulses, c) and d) propagation of waves.
$T_e/T_i = 1.0$, $v_d/c_i = 3$, $v_{dg}/c_i = 3$, $T_i/T_{ig} = 1$.

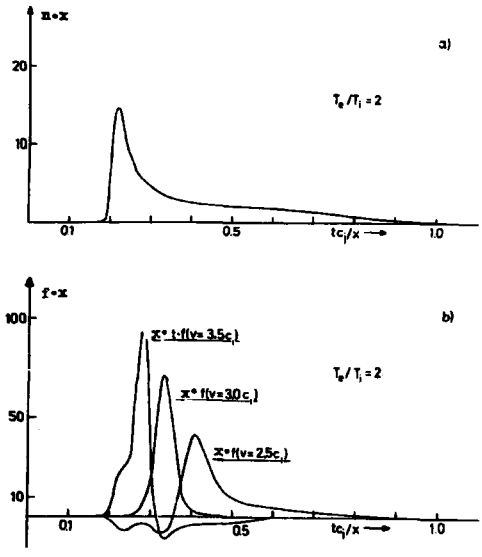

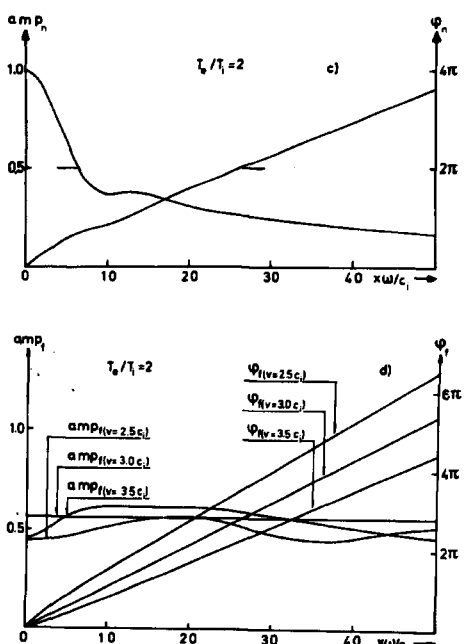

Fig. 4. a) and b) propagation of pulses, c) and d) propagation of waves.
$T_e/T_i = 2.0$, $v_d/c_i = 3$, $v_{dg}/c_i = 3$, $T_i/T_{ig} = 1$.

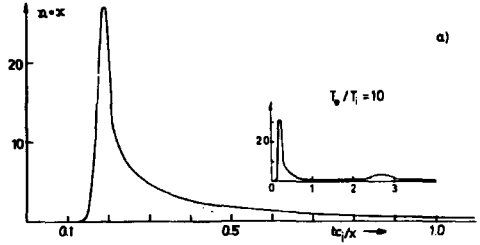

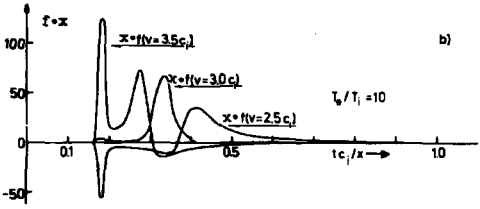

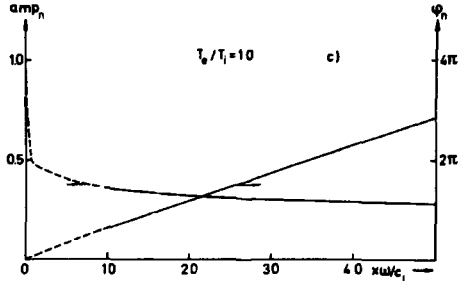

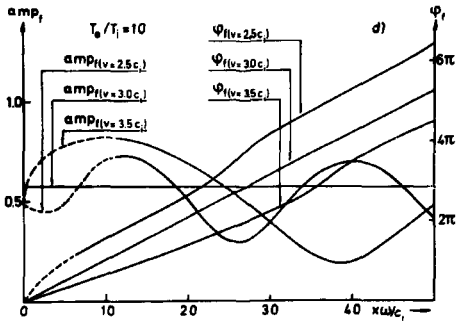

Fig. 5. a) and b) propagation of pulses, c) and d) propagation of waves. $T_e/T_i = 10.0$, $v_d/c_i = 3$, $v_{dg}/c_i = 3$, $T_i/T_{ig} = 1$.

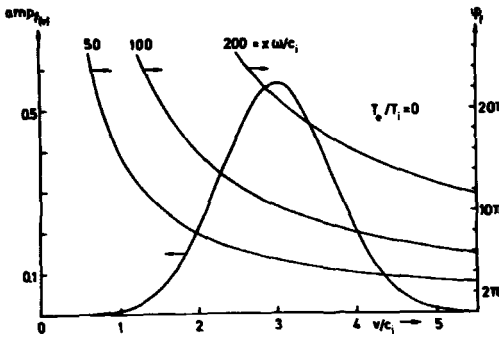

Fig. 6. Amplitude and phase of the perturbed ion velocity distribution function in a wave. $T_e/T_i = 0$, $v_d/c_i = 3$, $v_{dg}/c_i = 3$, $T_i/T_{ig} = 1$.

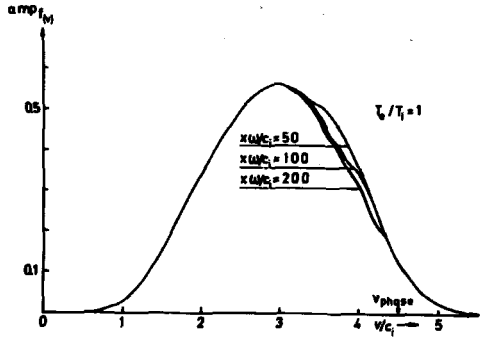

Fig. 7. Amplitude of the perturbed ion velocity distribution function in a wave at three distances from exciter. $T_e/T_i = 1$, $v_d/c_i = 3$, $v_{dg}/c_i = 3$, $T_i = T_{ig}$.

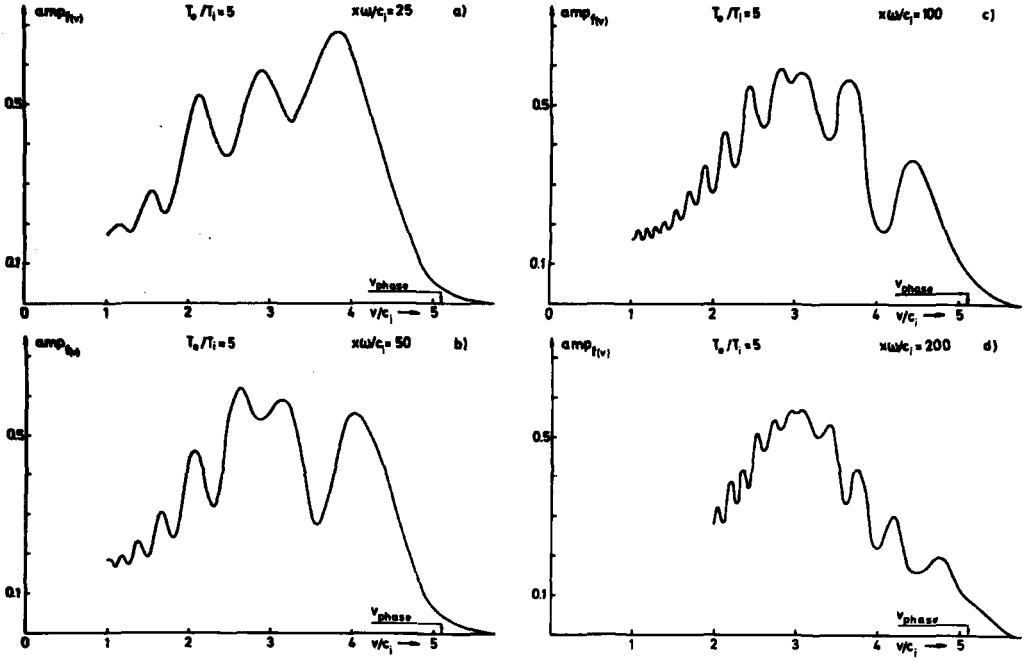

Fig. 8. Amplitude of the perturbed ion velocity distribution function in a wave at four distances from emitter. $T_e/T_i = 5$, $v_d/c_i = 3$, $v_{dg}/c_i = 3$, $T_i = T_{ig}$

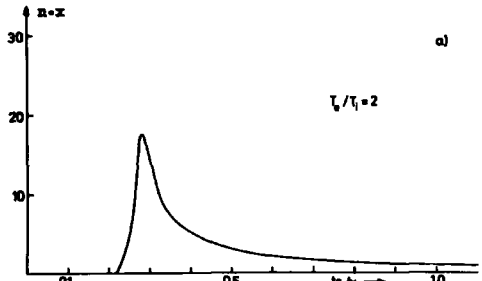

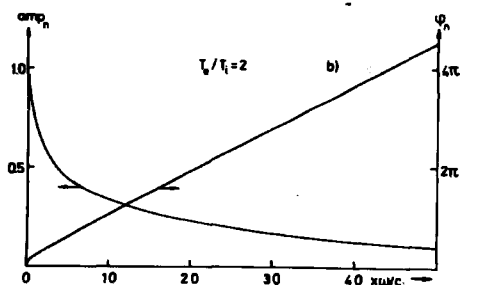

Fig. 9. a) propagation of pulses, b) propagation of waves. $T_e/T_i = 2$, $v_d/c_i = 2$, $v_{dg}/c_i = 2$, $T_i/T_{ig} = 1$.

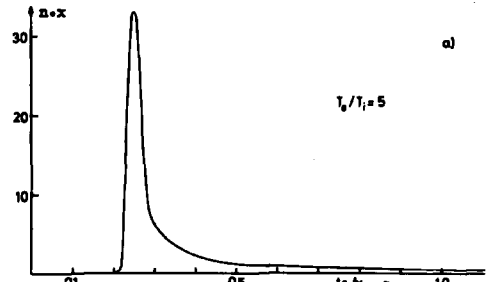

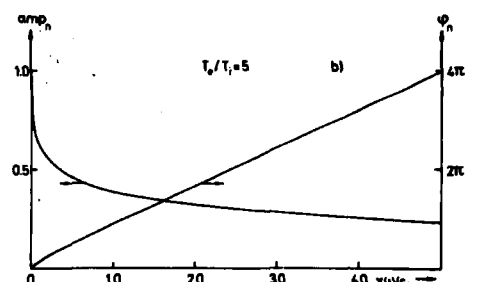

Fig. 10. a) propagation of pulses, b) propagation of waves. $T_e/T_i = 5.0$, $v_d/c_i = 2$, $v_{dg}/c_i = 3$, $T_i/T_{ig} = 1$.

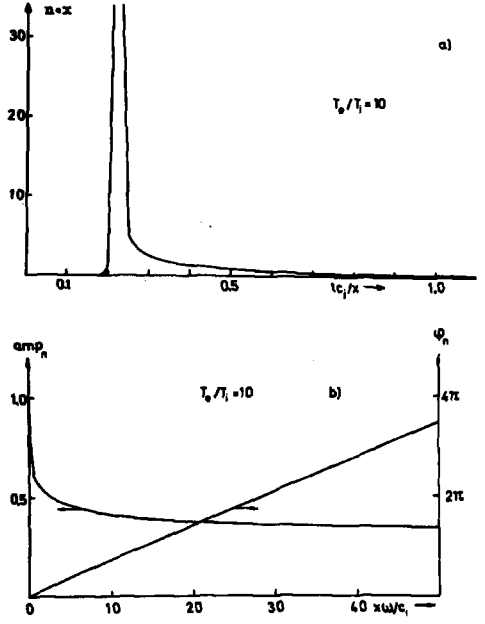

Fig. 11. a) propagation of pulses, b) propagation of waves. $T_e/T_i = 10.0$, $v_d/c_i = 2$, $v_{dg}/c_i = 2$, $T_i/T_{ig} = 1$.

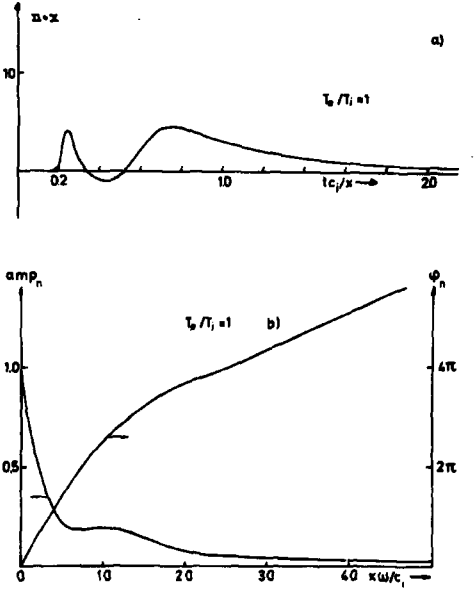

Fig. 12. a) propagation of pulses, b) propagation of waves. $T_e/T_i = 1.0$, $v_d/c_i = 3$, $v_{dg}/c_i = 1$, $T_i/T_{ig} = 1$.

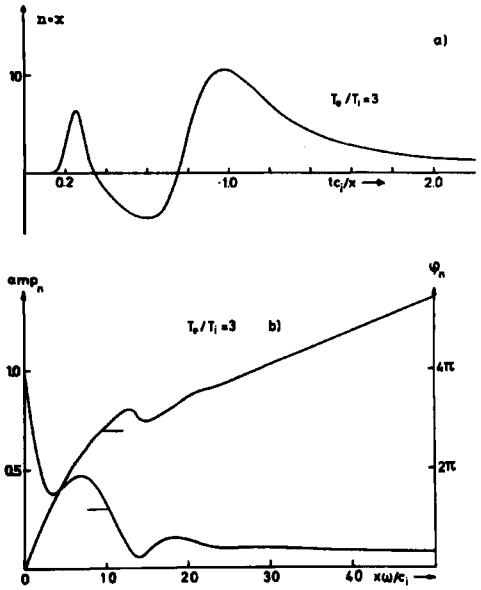

Fig. 13. a) propagation of pulses, b) propagation of waves. $T_e/T_i = 3.0$, $v_d/c_i = 3$, $v_{dg}/c_i = 1$, $T_i/T_{ig} = 1$.

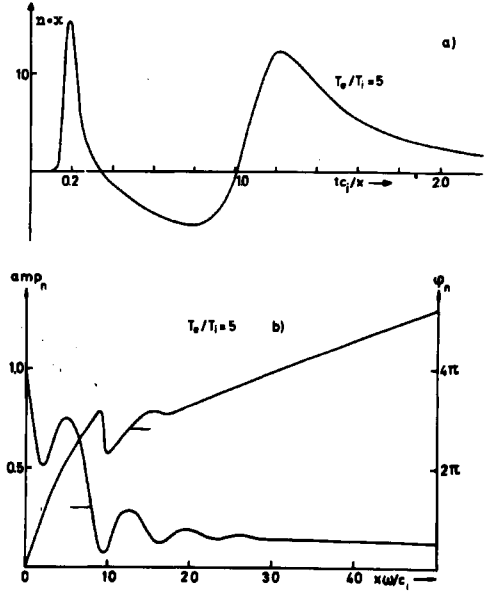

Fig. 14. a) propagation of pulses, b) propagation of waves. $T_e/T_i = 5.0$, $v_d/c_i = 3$, $v_{dg}/c_i = 1$, $T_i/T_{ig} = 1$.

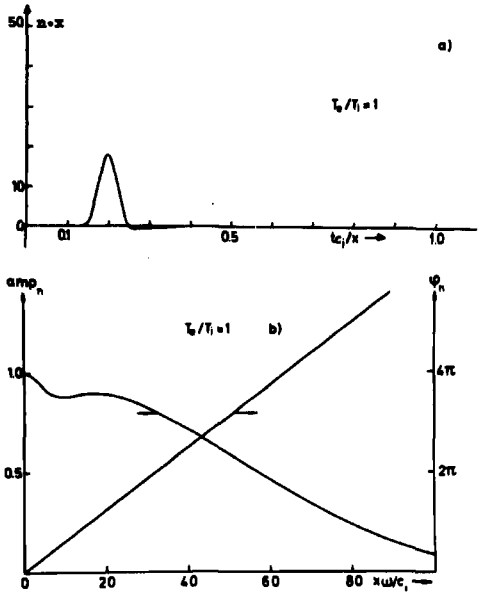

Fig. 15. a) propagation of pulses, b) propagation of waves. $T_e/T_i = 1.0$, $v_d/c_i = 3$, $v_{dg}/c_i = 5$, $T_i/T_{ig} = 1$.

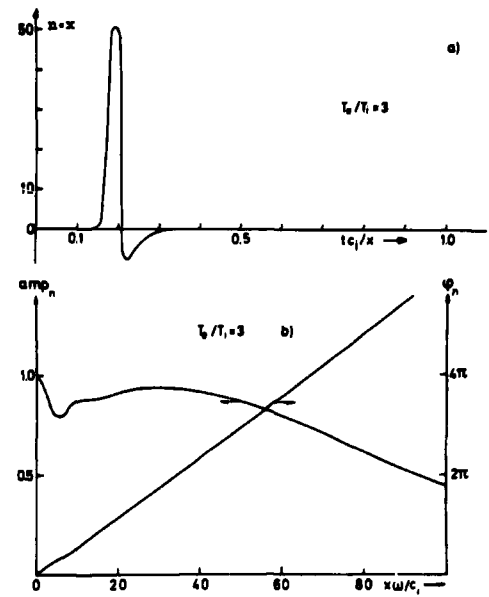

Fig. 16. a) propagation of pulses, b) propagation of waves. $T_e/T_i = 3.0$, $v_d/c_i = 3$, $v_{dg}/c_i = 5$, $T_i/T_{ig} = 1$.

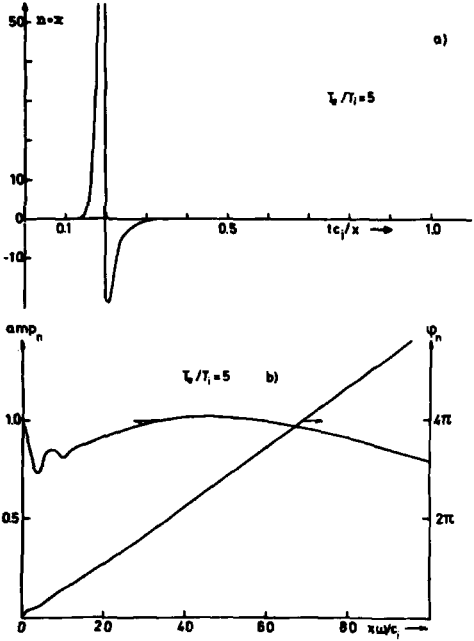

Fig. 17. a) propagation of pulses, b) propagation of waves. $T_e/T_i = 5.0$, $v_d/c_i = 3$, $v_{dg}/c_i = 5$, $T_i/T_{ig} = 1$.

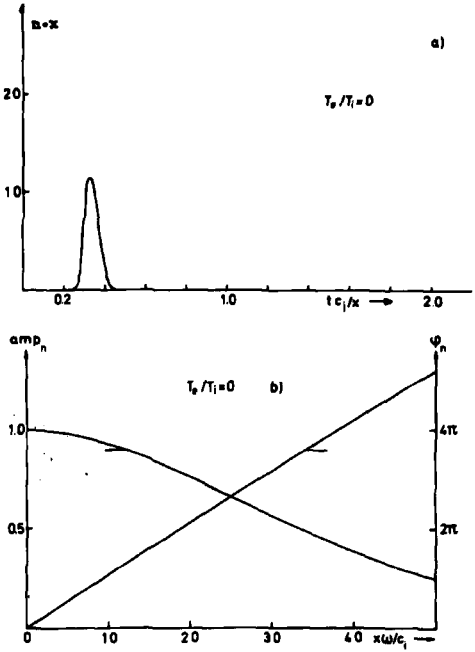

Fig. 18. a) propagation of pulses, b) propagation of waves. $T_e/T_i = 0.0$, $v_d/c_i = 3$, $v_{dg}/c_i = 3$, $T_i/T_{ig} = 5$.

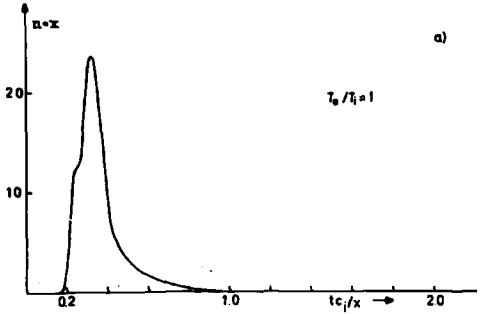

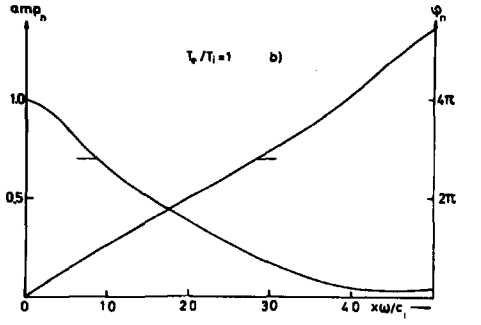

Fig. 19. a) propagation of pulses, b) propagation of waves. $T_e/T_i = 1.0$, $v_d/c_i = 3$, $v_{dg}/c_i = 3$, $T_i/T_{ig} = 5$.

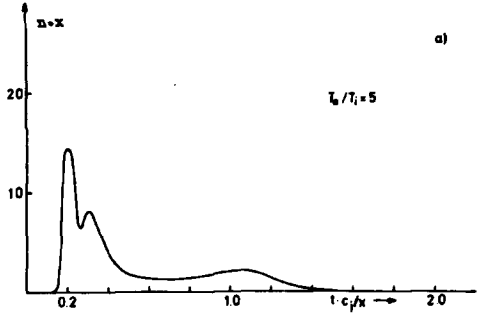

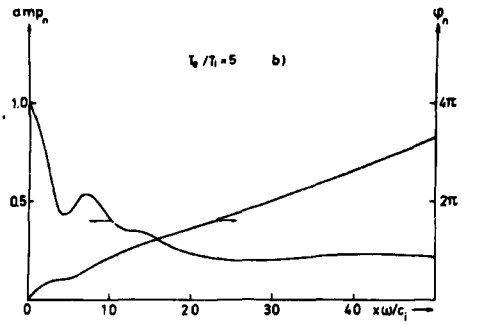

Fig. 20. a) propagation of pulses, b) propagation of waves. $T_e/T_i = 5.0$, $v_d/c_i = 3$, $v_{dg}/c_i = 3$, $T_i/T_{ig} = 5$.

$v_d/c_i = 3$, $v_{dg}/c_i = [illegible] T_i/T_{ig}$

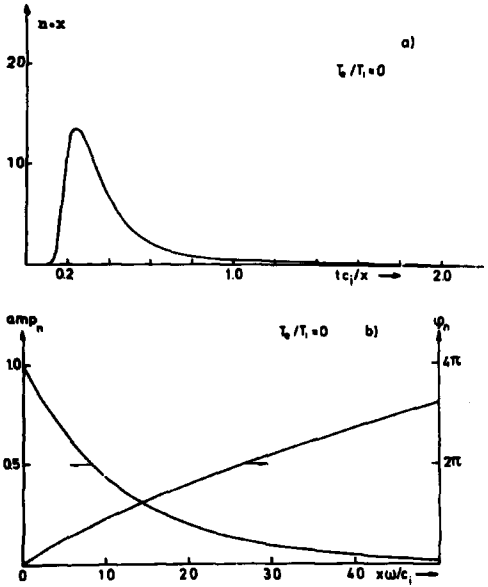

Fig. 21. a) propagation of pulses, b) propagation of waves. $T_e/T_i = 0.0$, $v_0/c_i = 3$, $v_{dg}/c_i = 3$, $T_i/T_{ig} = 0.2$.

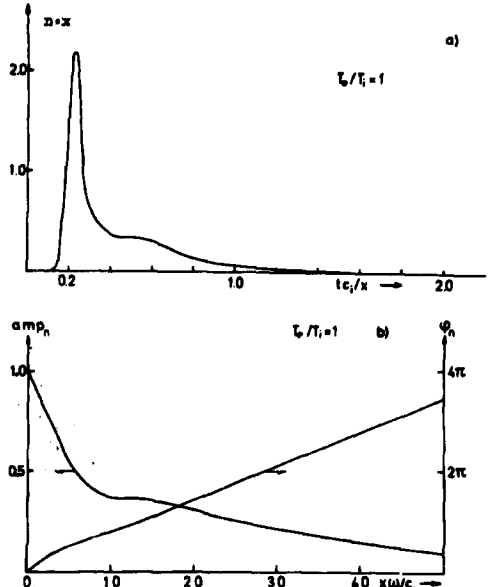

Fig. 22. a) propagation of pulses, b) propagation of waves. $T_e/T_i = 1.0$, $v_0/c_i = 3$, $v_{dg}/c_i = 3$, $T_i/T_{ig} = 0.2$.

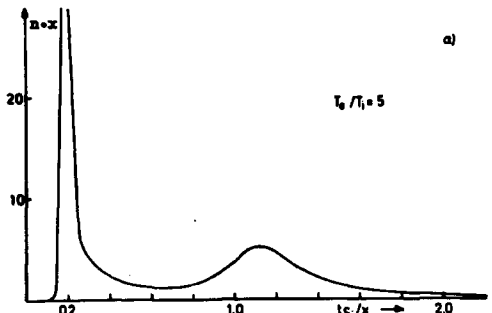

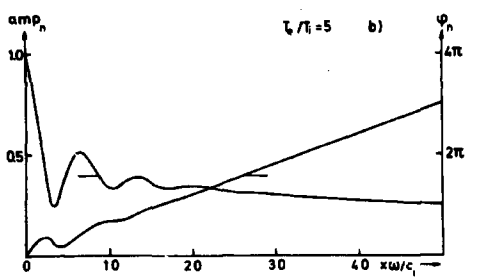

Fig. 23. a) propagation of pulses, b) propagation of waves. $T_e/T_i = 5.0$, $v_d/c_i = 3$, $v_{dg}/c_i = 3$, $T_i/T_{ig} = 0.2$.

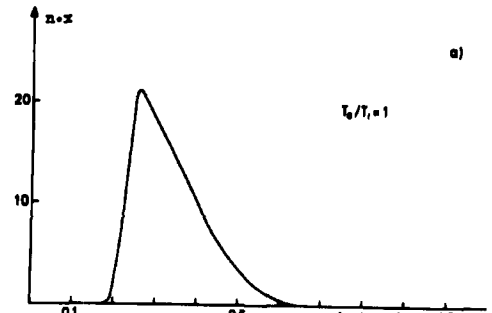

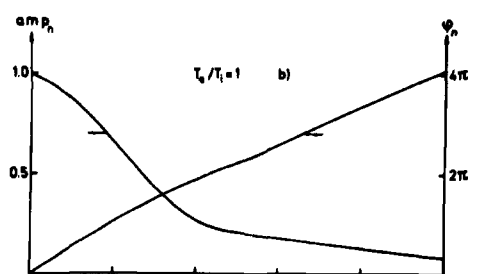

Fig. 24. a) propagation of pulses, b) propagation of waves. $T_e/T_i = 1.0$, $v_{d1}/c_i = 3$, $v_{dg}/c_i = 1$, $v_{dg}/c_i = 3$, $T_{i1} = T_{i2} = T_{ig}$.

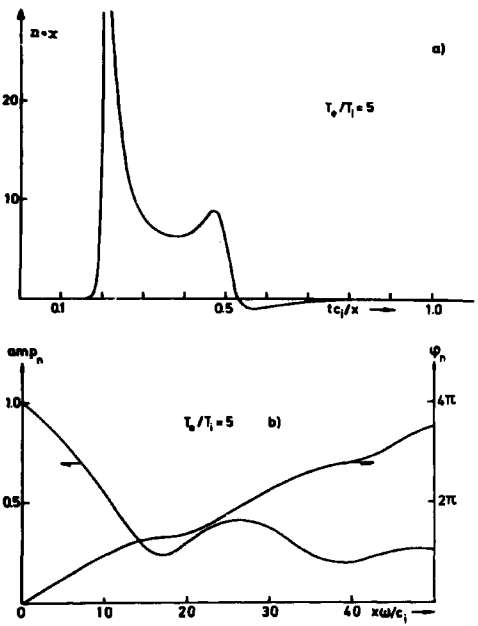

Fig. 25. a) propagation of pulses, b) propagation of waves. $T_e/T_i = 5.0$, $v_{d1}/c_i = 3$, $v_{d2}/c_i = 1$, $v_{de}/c_i = 3$, $T_{i1} = T_{i2} = T_{ig}$.

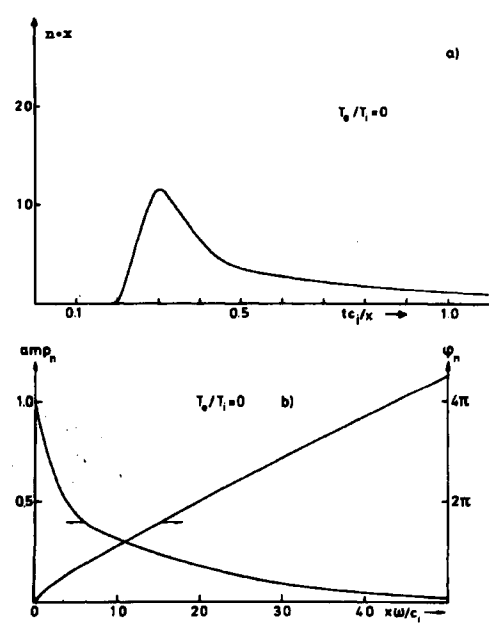

Fig. 26. a) propagation of pulses, b) propagation of waves. $T_e/T_i = 0.0$, $v_e/c_i = 3$, $v_{dg1}/c_i = 1$, $v_{dg2}/c_i = 3$, $T_i = T_{ig1} = T_{ig2}$.

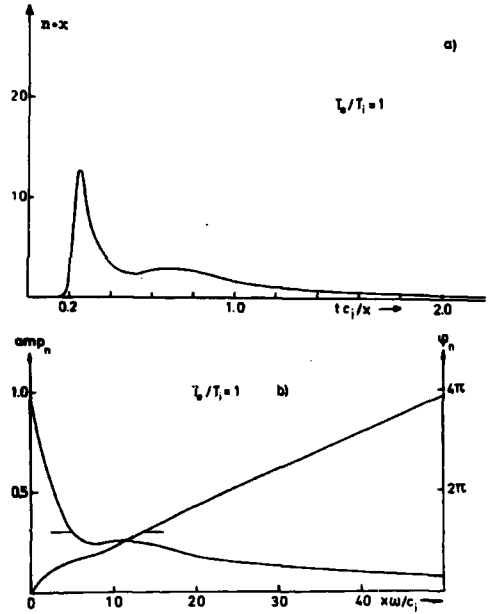

Fig. 27. a) propagation of pulses, b) propagation of waves. $T_e/T_i = 1$, $v_d/c_i = 3$, $v_{dg1}/c_i = 1$, $v_{dg2}/c_i = 3$, $T_i = T_{ig1} = T_{ig2}$.

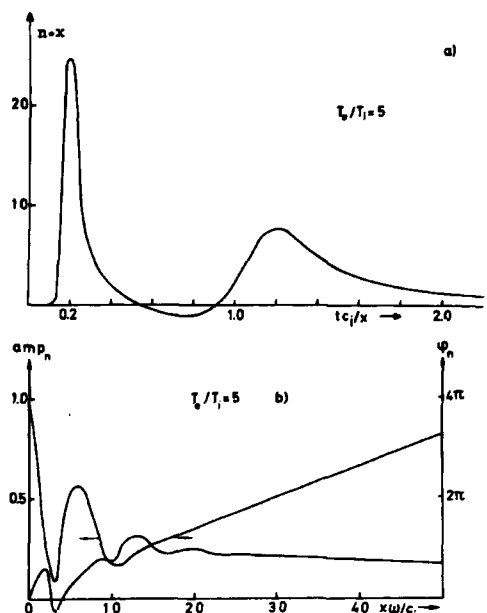

Fig. 28. a) propagation of pulses, b) propagation of waves. $T_e/T_i = 5$, $v_d/c_i = 3$, $v_{dg1}/c_i = 1$, $v_{dg2}/c_i = 3$, $T_i = T_{ig1} = T_{ig2}$.